JOURNAL OF CATALYSIS **54**, 207–218 (1978)

Preparation Variables in Nickel Catalysts

JAMES T. RICHARDSON AND REGIS J. DUBUS

Department of Chemical Engineers, University of Houston, Houston, Texas 77004

Received February 13, 1978; revised April 23, 1978

Nickel-on-silica catalysts were prepared by the homogeneous precipitation of slowly decomposing urea. After reduction the crystallite size distribution (CSD) of the nickel was determined from magnetic measurements. This technique was found to give very narrow CSDs and is much more reproducible than conventional impregnation methods. The nickel loading may be controlled by the solution concentrations and time of precipitation but higher values lead to broader distributions. The amount of reduced nickel is a function of the hydrogen flow rate and time, but these factors do not influence the CSD. Increasing reduction temperatures produce broader CSDs. Calcination has no effect on the resulting CSDs, nor does passivation in air after reduction. The uniform and stable crystallites resulting from this method are a consequence of the precipitation of nickel hydrosilicate homogeneously over the silica surface. This compound reduces slowly so that the metal does not sinter during reduction and small, uniform crystallites are produced.

Nickel catalysts are most effectively prepared through the optimal combination of high dispersion and metal loading (*1*). Small crystallite sizes ensure high specific metal areas, but increasing nickel concentrations result in agglomeration. The nickel surface area per unit volume of catalyst passes through a maximum, usually between 30 and 50 wt% (*2*). Even in the range below this maximum, common deposition procedures in impregnation and precipitation lead to inhomogeneous crystallite sizes, except for the least dilute samples (<5%). Increasingly broad and even bimodal crystallite size distributions (CSD) are found as the level of nickel increases. This not only changes the activity and selectivity patterns for demanding-type reactions but may also affect thermal stability, since resistance to sintering depends to some extent on the initial CSD (*3*). Preparation of catalysts with a small metal size and narrow CSD at high loadings is therefore an important objective in catalyst design.

Van Dillen and co-workers (*4*) recently reported a method for the homogeneous precipitation–deposition of nickel hydroxide on silica in aqueous suspension. The slow decomposition of urea in water above 343 K is a controlled source of hydroxyl ions. In the presence of nickel ions, these hydroxyls combine to precipitate nickel hydroxide slowly and homogeneously throughout the suspension. Furthermore, nickel hydroxide combines with silica upon precipitation to form a nickel hydrosilicate complex which is sufficiently immobile to be resistant to surface coalescence. Catalysts prepared in this manner exhibit a uniform dispersion of very small nickel particles (*4*).

Van Dillen *et al.* reported crystallites in the 1- to 2-nm-radius range but gave

0021-9517/78/0542-0207$02.00/0

no CSDs. We have used their method together with CSD measurements to investigate (a) the preparational parameters of precipitation time, solution concentration, and initial pH, (b) the reduction parameters of time, temperature, and flow rate, (c) the effect of calcining, (d) the effect of oxygen passivation, and (e) the effect of using alumina as the support.

The results, taken together with the chemistry of the precipitation and reduction processes, illustrate the variables of this potentially useful technique. In a later communication, we report a study of sintering phenomena and kinetics found in catalysts prepared in this way (*5*).

EXPERIMENTAL PROCEDURES

Catalyst Preparation

The reaction vessel was a 2-liter three-necked flask with a stirring rod in the center and a thermometer in the side neck. Urea was added to a suspension of silica or alumina in nickel nitrate solution after the heated solution reached 363 K, the temperature necessary to initiate precipitation. Deionized water and $Ni(NO_3)_2 \cdot 6H_2O$ and $(H_2N)_2CO$ (both reagent grade) were used together with silica (Cab-O-Sil HS5, 2.75×10^5 m^2/kg) or alumina (Catapal SB, activated, 2.50×10^5 m^2/kg).

In one series of experiments, the concentrations of nickel nitrate, urea, and the support were 0.14 *M*, 0.42 *M*, and 7.6 kg/m^3, respectively; in another series, 0.28 *M*, 0.84 *M*, and 10 kg/m^3. The initial pH was normally 4.0. In some cases, sufficient nitric acid was added to lower the pH to 2.5.

Changes in pH during precipitation are illustrated in Fig. 1. Curve (a) shows the effect of urea alone. At 363 K, the thermal decomposition of urea leads to carbon dioxide, ammonia, and hydroxyl ions. Most of the CO_2 dissolves as carbonate ions and the OH increases the pH, rapidly at first and then slowly, reaching a final pH of 7.0, which is expected for a weak acid–base mixture. With nickel nitrate present, the curve (b) follows the same initial increase but deviates at a pH of 5.8, when precipitation of nickel hydroxide begins. This process consumes hydroxyl groups as rapidly as they are formed so that the pH curve levels off at a lower value than before. The colloidal nickel hydroxide, although precipitated homogeneously, nucleates at

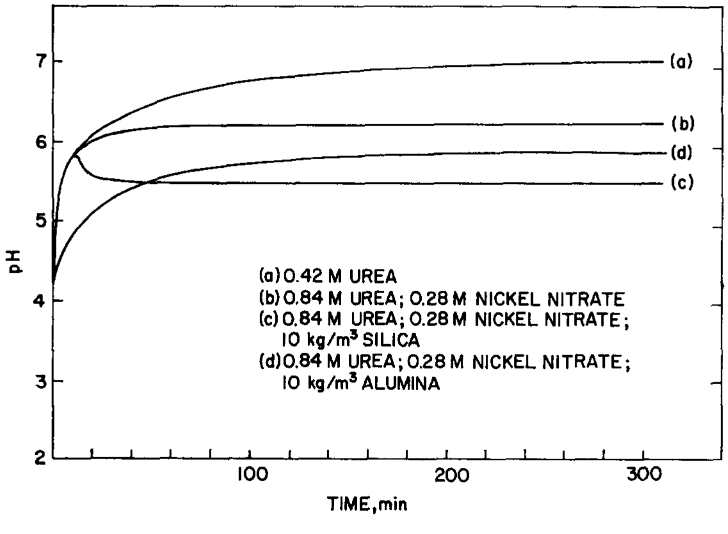

FIG. 1. Changes in pH during precipitation.

existing particles so that plate-like structures grow in size with time (*1*). Curve (c), with silica added, shows the effect of strong support interactions. Precipitation occurs rapidly at sites on the silica surface so that the pH drops after passing through a maximum. Precipitation and nucleation then occur only on the silica and not in the solution. The precipitated species is adsorbed securely enough to resist migration so that continued deposition results only in a highly dispersed nickel hydrosilicate, $Ni_3(OH)_4Si_2O_5$. This process continues with dissolution into the silica particle itself (*4*).

Up to 46 wt% nickel the solid contains increasing amounts of the hydrosilicate. Samples prepared at a precipitation time greater than 8 hr had a noticeably lower bulk density, showing the onset of peptization promoted possibly by the accumulation of excess hydroxyl ions.

Alumina behaves differently. Precipitation occurs earlier, consuming the hydroxyl groups as rapidly as they are formed. The maximum, characteristic of strong support interaction, is not observed. Nucleation continues on deposited nickel hydroxide particles so that these samples are expected to yield lower dispersions of nickel.

Samples with increasing amounts of total nickel were prepared by allowing precipitation to proceed for longer times. To stop the reaction, the heating mantle was removed and the suspension cooled while stirring. The green precipitate was filtered and washed with hot water. The catalyst was dried in an oven at 393 K overnight and crushed to less than 0.025-cm-diameter particles.

The total nickel content on each sample was determined by a colorimetric method described by Coenen and Linsen (*6*).

Although most samples were used as prepared, some were calcined in air at various temperatures and times.

Reduction Procedures

The catalysts were treated (reduced, cleaned, calcined, etc.) in the same cell used for magnetic measurements. The cell is illustrated in Fig. 2. The outer 12-mm quartz tube contained 1 cm of catalyst. Reducing and purge gases passed through the inner capillary tube. In some cases, the outer fixtures were ground joints and stopcocks; in others, Cajon fittings and valves were used.

Each sample was weighed (2 to 8 × 10^{-4} kg), charged to the cell, and then connected to a gas handling system with a sleeve furnace in position. High purity grade hydrogen was passed through the bed at a flow rate from 25 to 200 cm^3/min and the temperature raised to reduction temperatures at a rate of 8°/min.

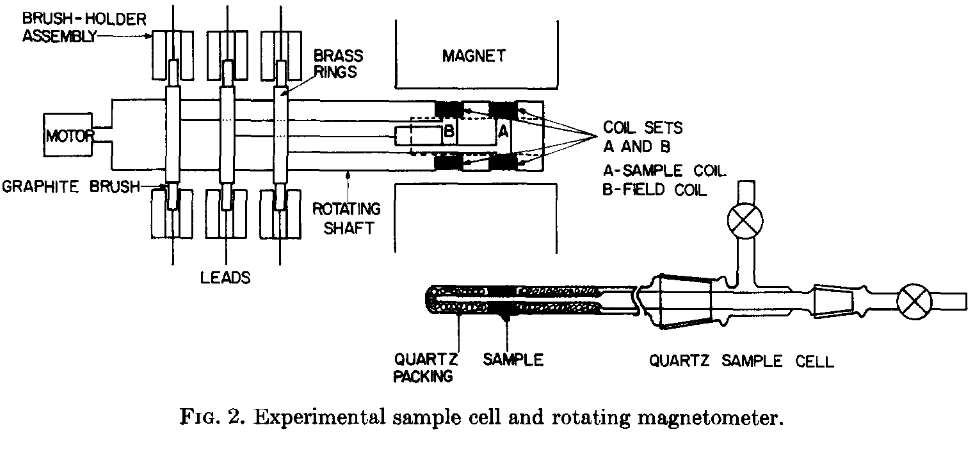

FIG. 2. Experimental sample cell and rotating magnetometer.

At the completion of reduction, the sample was outgassed in purified argon or helium for 1 hr at 25° above the reduction temperature to remove absorbed hydrogen. It was cooled to ambient temperature with the inert gas still flowing.

The cell was then transferred to the magnetometer for magnetization measurements.

Magnetization Measurements

In this study, magnetization measurements were made with a low-field electromagnet at fields less than 9 kOe. The magnetometer was a rotating coil device, shown in Fig. 2. The 1-cm catalyst bed in the quartz cell was positioned in the hollow polystyrene shaft with the sample between two 500-turn coils connected in series. These sample coils were connected in opposition to an equivalent set of field coils, all within the magnetic field. An ac motor rotated the shaft at 30 Hz. Each coil set generated a sinusoidal signal proportional to the magnetic induction between them. When connected differentially, the signal was a measure of the sample magnetization. The ac signal was filtered, amplified, and measured with a digital voltmeter. Voltages up to 10 mV were recorded with a precision of ±0.05 mV.

Samples of nickel powder, appropriately diluted, were used to measure a linear calibration curve from which the absolute magnetization, M, was found for each voltage. The field coil gave a voltage proportional to the magnetic field, H, with a precision of ±3 Oe.

Figure 3 demonstrates the measured voltage–magnetic field curve for a typical sample. The CSD computation is based on an analysis of the M/M_s curve, where M_s is determined by extrapolation to infinite fields if data are obtained close to saturation. This is inaccurate for highly dispersed samples without ultrahigh fields or low temperatures. We overcame this difficulty by sintering the sample in helium at 1100 to 1200 K for a sufficient time to achieve magnetic saturation at low fields. Care was taken to avoid problems associated with this approach (*7*). Ultrapure helium was further cleaned by the use of a guard chamber of high-nickel catalyst. This effectively removed all contamination from

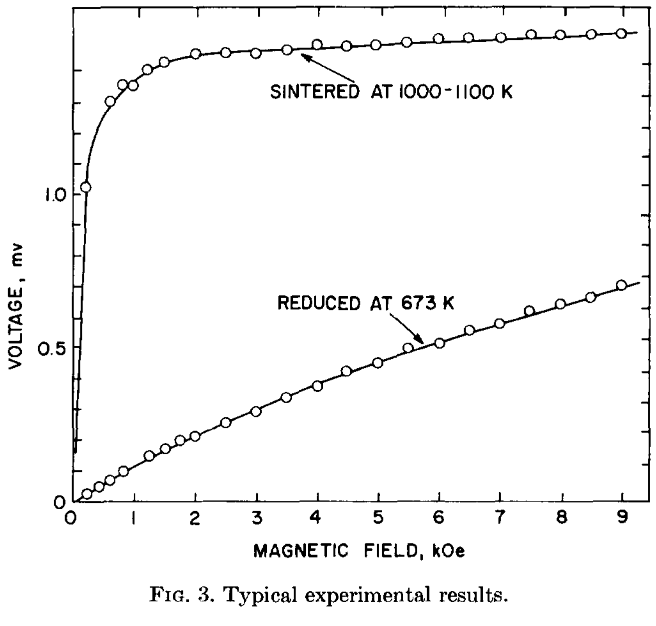

FIG. 3. Typical experimental results.

TABLE 1

Effect of Preparational Parameters

Parameter	CSD	Effect on extent of reduction
Method		
Homogeneous precipitation	Small, narrow	Moderate
Impregnation	Broad, bimodal	High
Precipitation		
Time	Increases	None
Solution concentration	Increases	Increases
Initial pH	Increases slightly	Decreases
Reduction		
Time	None	Increases
Temperature	Increases	Increases
Flow rate	None	Increases
Calcination	None	None
Passivation	None	None
Support		
Silica	Narrow	Moderate
Alumina	Bimodal	High

the gas. No oxidation from the support was encountered with the silica, although this may be a problem with alumina, as well as loss of nickel through compound formation. However, a complication did arise with silica when it was found through X-ray analysis that the unreduced nickel hydrosilicate decomposes at high temperatures to give easily reduced nickel oxide. Accordingly, the sintered sample was not exposed to hydrogen since this could have resulted in the reduction of additional nickel.

The value of M_s also gave the amount or fraction of reduced nickel in the sample (*8*).

Computations of Crystallite Size Distribution

The CSDs were computed with techniques previously reported (*8*). Low fields were used for convenience, although some sacrifice in precision was expected. The extent of this was examined with model distributions in which various functions were used to calculate magnetization curves and CSDs were computed for comparison of high and low field methods.

In all cases, a high degree of precision was found when data up to 80 kOe were used. For the low field range, narrow distributions centered at a radius of less than 1.5 nm were less accurate in shape, although qualitatively the locations and spread were fairly accurately given. As the mean radius or variance increased, the agreement improved. If the CSDs for very small crystallites are accepted as qualitatively correct and not too much emphasis placed on shape, then the results of this study are accurate enough for the conclusions made.

RESULTS AND DISCUSSION

The main purpose of this investigation was to assess the effect of preparational parameters on the CSD and extent of reduction. Parameters examined and the conclusions reached are summarized in Table 1 and a detailed discussion follows.

Homogeneous Precipitation–Deposition

Figure 4 shows a comparison between samples prepared by urea precipitation and impregnation with nickel nitrate. Both samples contained about the same amount of total nickel and were reduced under identical conditions (15 hr at 673 K) yet the precipitation CSD is very narrow and small compared to the result of the impregnation. Clearly, the expectations of the method have been achieved. The distributions and sizes shown are typical of the best results with this technique. Most of the crystallites are from 1 to 2 nm in radius. None of the samples with relatively high loadings had a mean radius of less than 1.0 nm.

The precipitation procedure is also extremely reproducible. For example, two separate preparations (with different operators following identical recipes) of the sample in Fig. 4 resulted in almost identical CSDs and reductions. Impregnation, however, was very difficult to repeat. Even specimens from the same preparation were different.

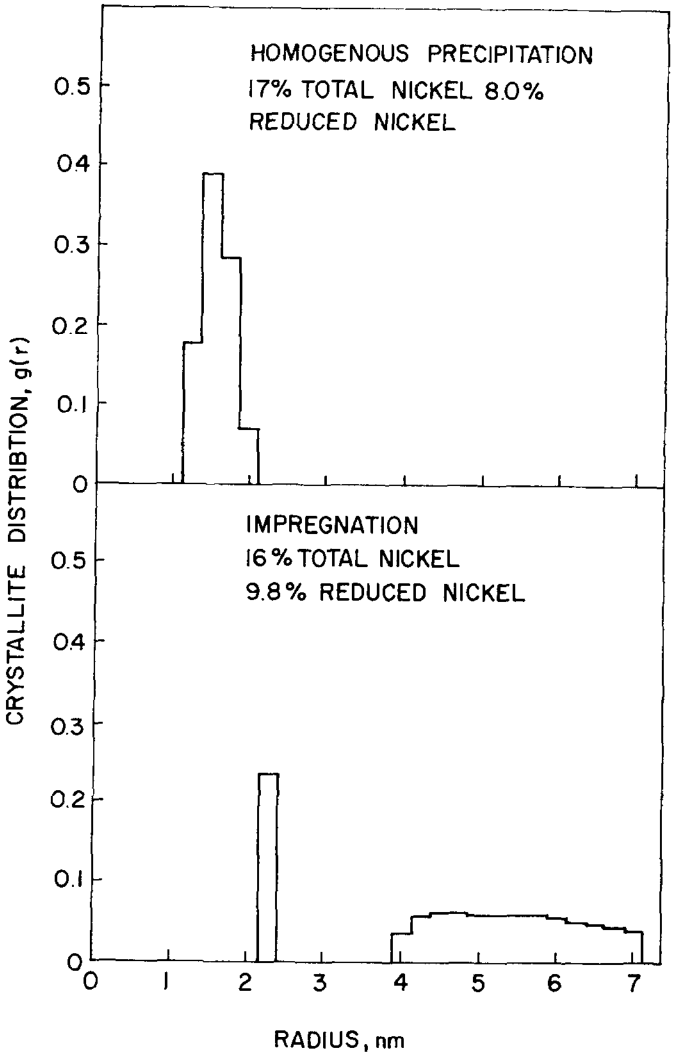

Fig. 4. *Effect of method of deposition.*

Effect of Precipitation Time

The effect of precipitation time is to increase the total amount of nickel deposited, as shown in Fig. 5.

The extent of reduction is approximately the same for these samples (29–35%), suggesting that a uniform layer of nickel hydrosilicate of increasing thickness is formed over the silica. Even at 25% total nickel, a considerable fraction of the particle is nickel hydrosilicate. Upon reduction the layer breaks up into nickel crystallites separated by silica and supported on unreduced nickel hydrosilicate. Increasing thickness of the original layer results in larger and inhomogeneous crystallites, due to a greater opportunity for further nucleation around the metal as reduction progresses.

From these and subsequent results, we conclude that the nickel concentration is much more important in determining the CSD than is the amount of reduced metal. This implies that crystallite growth during reduction is a consequence of nucleation and not sintering, at least up to 673 K.

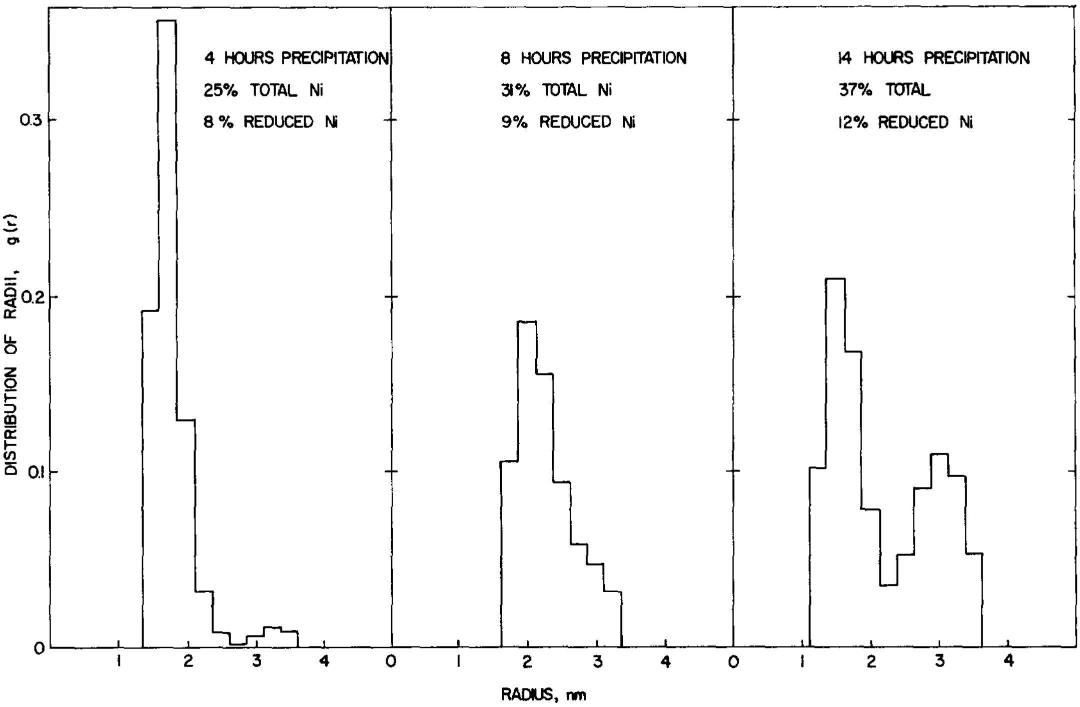

Fig. 5. Effect of precipitation time.

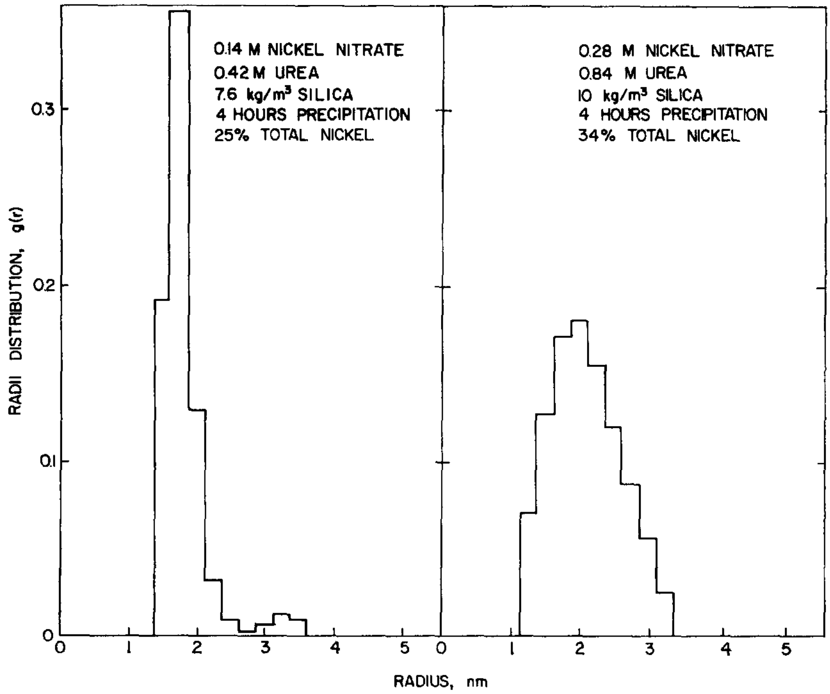

Fig. 6. Effect of solution concentrations.

Effect of Solution Concentrations

Increasing the concentrations of urea and nickel nitrate resulted in increased nickel deposition, leading to decreased dispersion. Differences in CSD are illustrated in Fig. 6.

The effect of precipitation time on the CSD was much less for the higher concentrations, possibly because the amount of nickel deposited reached a steady value for the longer times. One difference is significant. The extent of reduction was higher and increased with time although the total nickel content did not change significantly. Longer aging at these conditions may have resulted in differences in the sample texture, helping the reduction process.

Effect of Initial pH

This variable was explored in only one experiment. Two samples were prepared with 4 hr of precipitation from 0.4 *M* urea solution, but sufficient nitric acid was added to one of them, lowering the initial pH from 4 to 2.5. The result was a slightly lower CSD with less total nickel for the sample with lowered pH. However, the extent of reduction increased, showing some effect on the deposition mechanism.

Effect of Reduction Time

Figure 7 shows the effect of time on reduction at 673 K. The CSD is remarkably uniform but the extent of reduction increases. Sintering does not appear to have involved the reduction in any way. Initially, the reduction occurred at a fast rate so that about 30% of the nickel was reduced at 5 hr. Thereafter the process was slower. This may indicate rapid reduction of the outer layer of nickel hydrosilicate followed by slower reduction deeper in the particle.

The uniformity of the CSDs implies that the sites of reduction nucleation are homogeneous throughout.

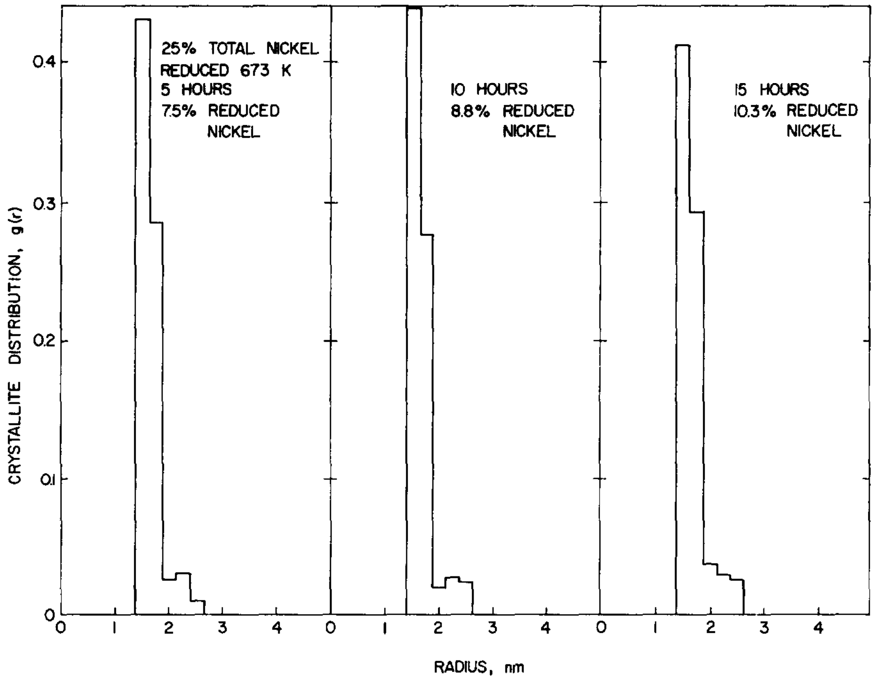

FIG. 7. Effect of reduction time.

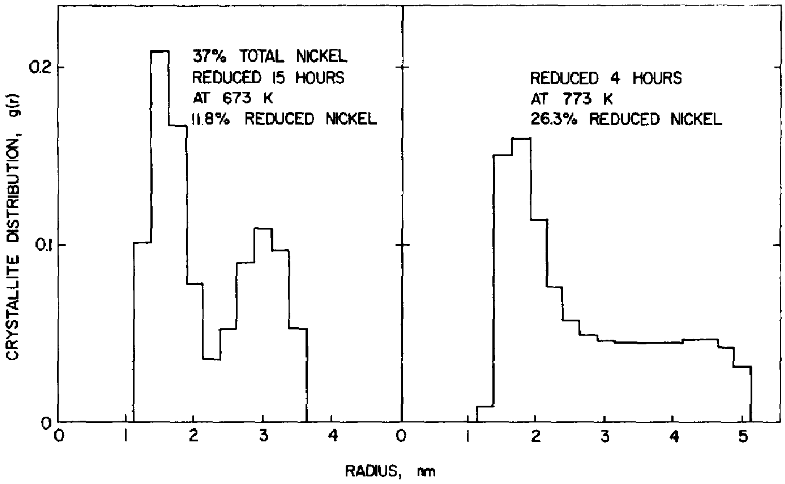

FIG. 8. Effect of reduction temperature.

Effect of Reduction Temperature

Reduction at temperatures higher than 673 K resulted in broader CSDs, as shown in Fig. 8. Many of the samples had bimodal distributions. These effects may have come from accelerated sintering during reduction or from the reduction of separate precursors which are harder to reduce at lower temperatures yet result in larger crystallites.

Effect of Hydrogen Flow Rate

Figure 9 demonstrates the dependence of the extent of reduction on hydrogen gas velocity. The CSDs are again unchanged. Particle Reynolds numbers at these conditions are extremely small (0.01–0.05) so that the flow is almost in the Stokes region, yet the mass transfer coefficient for hydrogen is six orders of magnitude higher than the fastest reduction rate. The reduction process generates almost 2 mol of water for every mole of nickel so that the presence of moisture may impede the thermodynamic equilibrium conversion of the nickel. The equilibrium ratio of H_2O/H_2 at 673 K is about 15, as calculated from bulk thermodynamics. This seems to be sufficiently high to exclude this explanation except that higher concentrations could exist in the microporous structure of the nickel silicate layers. This, in turn, would also decrease the hydrogen diffusion from the external gas. As the velocity increases, the removal of water vapor is facilitated, with a corresponding increase in reduction rate.

The reduction step may follow decomposition of the nickel silicate to the oxide, perhaps controlled by the same water removal. These factors will be explored in further investigations.

Varying the hydrogen flow rate was found to be a very sensitive and reproducible method of controlling the amount of reduced nickel.

Effect of Calcination

Calcination in air prior to reduction has little effect on the resulting CSD. Temperatures from 623 to 723 K were tried with similar results. This implies that the reduction precursor, presumably nickel hydrosilicate, is not drastically altered by the air treatment. This is in contrast to other systems, such as alumina, where calcination promotes support compound formation (*11*).

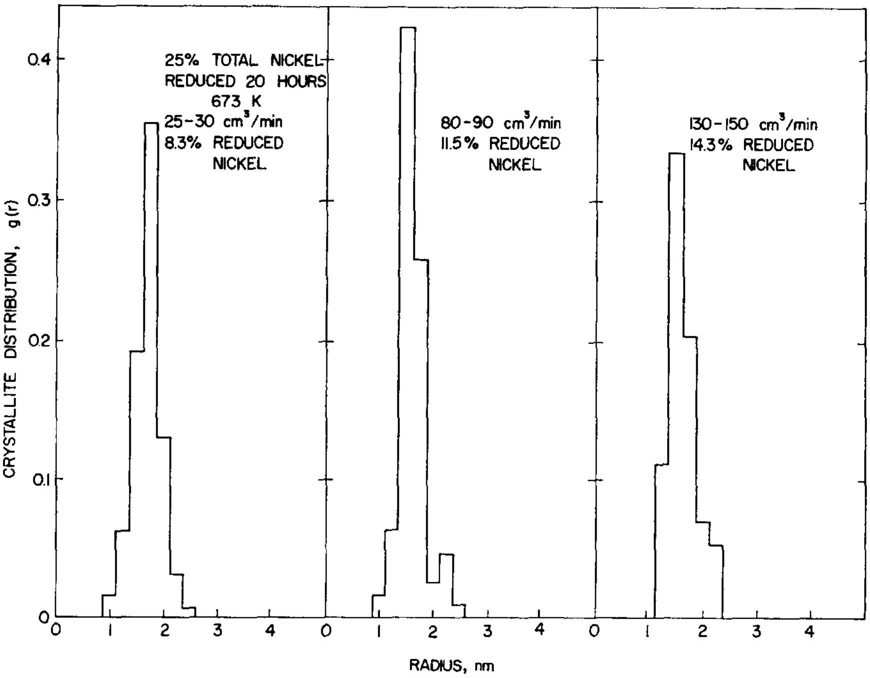

FIG. 9. Effect of hydrogen flow rate.

Effect of Passivation

Reduced nickel catalysts are often passivated by treatment in dilute oxygen to protect the nickel during subsequent handling operations. In order to check whether or not this procedure alters the resulting CSD, we performed the following experiment.

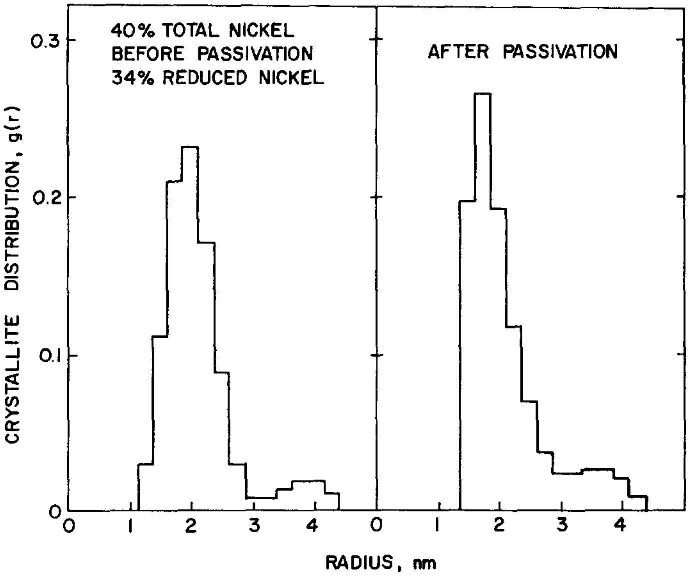

FIG. 10. Effect of passivation.

A sample was reduced and cleaned in the usual manner, and the magnetization curve taken. A 2% mixture of air in helium was passed over the catalyst at 298 K for 1 hr. The air concentration was then increased slowly to 1 atm and the sample cell exposed to the laboratory atmosphere overnight. Subsequent reduction and measurement resulted in the CSDs shown in Fig. 10. They are identical within experimental error.

Some interesting observations were made about the pyrophoric nature of dispersed nickel. After a reduced catalyst had been cleaned in argon at 25 K above the reduction temperature, the magnetization curve increased about 30%. Adsorption of hydrogen at room temperature returned the curve to its postreduction value, implying that, prior to cleaning, the surface is saturated with hydrogen. At this point the catalyst was exposed to air and rapid oxidation and heating of the catalyst followed. The dispersion of the nickel was destroyed by the exothermic heat of oxidation. However, exposure of the catalyst to air after cleaning produced no temperature increase and the magnetization curve showed a decrease consistent with the adsorption of a monolayer of oxygen (*10*). Further reduction, cleaning, and measurement gave a CSD almost identical with the nonoxidized sample.

These results confirm the observation of Popowicz *et al.* (*11*) that the adsorbed hydrogen and not the nickel initiates the dangerous pyrophoric oxidation of the nickel. Thus, only proper cleaning operations are necessary in order to protect the catalyst bed prior to removal from the reactor or after reduction. Admission of air, however, should still be slow and controlled in case some hydrogen remains adsorbed.

Effect of Support

Comparisons of the results of silica and alumina supports are shown in Fig. 11. Alumina does not perform as well in developing a narrow and small CSD. It is therefore not as good a candidate for the technique.

CONCLUSIONS

The homogeneous deposition–precipitation of nickel on silica has been shown to generate narrow and reproducible crystallite size distributions. Time of precipitation is the most important factor, with longer times leading to higher nickel loadings

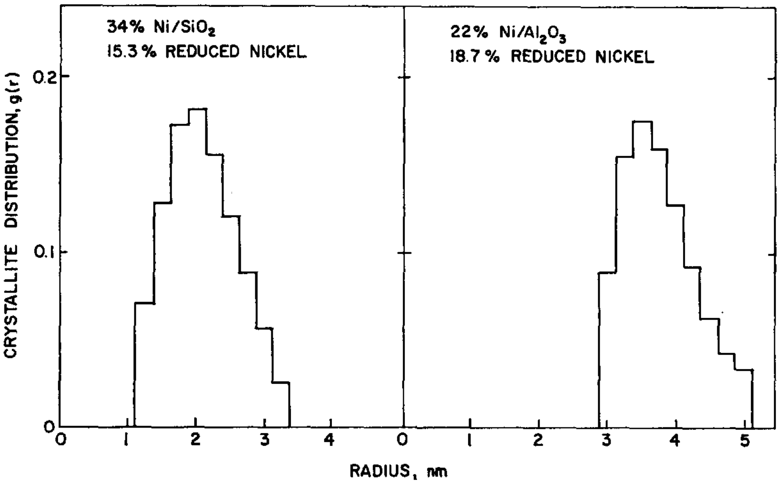

FIG. 11. Effect of support.

and broader distributions after reduction. Nevertheless, high dispersions up to 30 to 40 wt% are possible.

The CSD of the nickel is independent of the degree of reduction at a given temperature but shows the effect of secondary sintering at temperatures above 723 K. The amount of reduced nickel may be controlled by the hydrogen velocity. Calcination and passivation have little effect on the CSD.

The key to this behavior appears to be the metal nucleation of nickel hydrosilicate, which reduces slowly to highly dispersed and uniform nickel crystallites. Sintering studies in this laboratory are reported in another communication and show that the catalyst is very resistant to crystallite growth.

This technique is a suitable method for the control of CSDs. Scale-up to commercial processes should be possible.

ACKNOWLEDGMENTS

The authors are indebted to the Robert A. Welch Foundation for support of this research. The cooperation of their colleagues, P. Desai and J. G. Crump, is gratefully acknowledged.

REFERENCES

1. Geus, J. W., "Sintering and Catalysis," (G. C. Kuczynski, Ed.), p. 29. Plenum Press, New York, 1975.

2. Dixon, G. M., and Singh, K., *Trans. Farad. Soc.* **65**, 1128 (1969).

3. Flynn, P. C., and Wanke, S. E., *J. Catal.* **34**, 290 (1974).

4. Van Dillen, J. A., Geus, J. W., Hermans, L. A. M., and Van Der Mejden, "Proceedings of the Sixth International Congress on Catalysis," Paper B7, July 1976, London.

5. Richardson, J. T., and Crump, J. G., to appear.

6. Coenen, J. W. G., and Linsen, B. F., "Physical and Chemical Aspects of Adsorbents and Catalysts." Academic Press, New York, 1970.

7. Carter, J. L., Cusumano, J. A., and Sinfelt, J. H., *J. Phys. Chem.* **70**, 2257 (1966).

8. Richardson, J. T., and Desai, P., *J. Catal.* **42**, 294 (1976).

9. Richardson, J. T., and Milligan, W. O., *J. Phys. Chem.* **60**, 1223 (1956).

10. Dalmon, J. A., Martin, G. A., and Imelik, B., *Surface Sci.* **41**, 587 (1974).

11. Popowicz, M., Celler, W., and Treszczanowicz, E., *Int. Chem. Eng.* **6**, 63 (1966).